Revealing Successive Steps of Deprotonation of L- Phosphoserine through ^{13}C and ^{31}P Chemical Shielding Tensor Fingerprints

Carole Gardiennet-Doucet,[†] Xavier Assfeld,[‡] Bernard Henry,[§] and Piotr Tekely*[,†]

Méthodologie RMN, Chimie et Biochimie Théoriques, and Chimie-Physique, UMR CNRS 7565, Université Henri Poincaré, Nancy 1, 54506 Vandoeuvre-lès-Nancy, France

Received: April 7, 2006; In Final Form: May 31, 2006

The effects of deprotonation on the ^{13}C and ^{31}P chemical shielding tensors of L-*O*-phosphoserine are revealed by using solid-state NMR spectroscopy and ab initio calculations. The characteristic changes in some principal elements of the ^{13}C and ^{31}P chemical shift tensors have been detected during successive steps of deprotonation of carboxyl, phosphate, and amide functional groups. The calculations carried out in a polarizable continuum taking into account the effects of the surroundings have shown their ability to reproduce correctly the changes of the principal values induced by deprotonation and to provide precious information, which is very difficult to obtain experimentally, about the concurrent changes in the orientation of chemical shielding tensors in the molecular frame. The experimentally observed subtle effects related to the deprotonation-induced modifications of intermolecular contacts involving hydrogen bonding as well as the influence of counterions on the ^{13}C and ^{31}P principal elements of the chemical shift tensors are also discussed.

Introduction

A straightforward assignment and characterization of charges and hydrogen bonding neighborhood for ionizable species such as carboxyl, amino, phenolic, and imidazole groups found in proteins remains a challenging problem in the elucidation of a mechanism for proton transfer reactions in solids and membrane proteins including the bacteriorhodopsin photocycle and ATP synthetase. An equally important issue when analyzing kinases and phosphatases at the molecular level or the activation of biomolecules is whether a phosphate group is mono- or dianionic.

Solid-state ^{13}C and ^{31}P NMR determinations of the acid−base ratios of lyophilized compounds allow the accurate measurements of the p*K* values of successive deprotonations, without recourse to full titration curves.[1] The obvious advantage of solid-state over liquid-state NMR spectroscopy arises from a dramatic slowing down of inter- and intramolecular proton exchanges on the NMR time scale and from an easy access to the principal values of chemical shift anisotropy (CSA) tensors, which, by virtue of their nature, are much more sensitive to changes in the ionization state and hydrogen bonding interactions than isotropic chemical shifts. Indeed, the chemical shift tensor is known to be an extremely valuable source of information about the local electronic environment of a nucleus and its local site symmetry.

The experimentally obtained principal values of the chemical shift anisotropy provide a sensitive test of modern molecular quantum mechanical calculations of chemical shielding. Somewhat surprisingly, the calculations of the chemical shielding tensors upon deprotonation have not been so far presented in the literature.

In this work we report ^{13}C and ^{31}P solid-state NMR and the density functional theory (DFT) studies of deprotonation (Scheme 1) of L-phosphoserine, playing a crucial role in enzymatic chemistry. The main aims of our work are to detect and analyze the spectroscopic fingerprints from the ^{13}C and ^{31}P chemical shift tensors upon deprotonation of L-phosphoserine and to provide further support for our recent findings[1b,c] of the exceptional suitability of chemical shift tensor for a straightforward determination of the ionization state following successive deprotonations of different functional groups. We also wish to appreciate the extent of concurrent influence of changing intermolecular contacts involving hydrogen bonding and counterions on the ^{13}C and ^{31}P principal elements of the chemical shift tensors.

Experimental Section

1. Lyophilization. A sample of L-*O*-phosphorylated serine (Sigma-Aldrich) was dissolved in bidistilled water, and the volume was adjusted to 10 mL (0.1 M solution). The pH value was adjusted with NaOH at 25 °C using an Orion 901 pH meter equipped with an Orion 91-03 electrode that was previously standardized with appropriate buffer solutions. Samples were frozen in a 50 mL rotating flask immersed in liquid nitrogen to obtain a thin solid layer with a large surface area. The flask was then detached from the rotating system and fitted to a lyophilizator for 6 h at −80 °C and 300 Pa.

2. Solid-State NMR Experiments. All experiments were carried using a Bruker Avance-300 NMR spectrometer. A 4 mm double resonance magic-angle-spinning (MAS) probe tuned to ^{13}C and ^{31}P frequencies at 75.46 and 121.46 MHz, respectively, was used. The single-pulse or CP/MAS NMR spectra (using the contact time between 1 and 3 ms) were recorded in the presence of phase-inversion high-power proton decoupling.[2] The number of scans was 400 and 64 for the ^{13}C and ^{31}P, respectively. The ^{13}C chemical shifts were measured indirectly by reference to the carbonyl α-glycine line set at 176.5 ppm; the ^{31}P chemical shifts were calibrated indirectly through bis-(dineopentoxyphosphorothioyl) disulfide set at 84.0 ppm. The principal values of the chemical shift anisotropy tensors were

* Corresponding author. E-mail: piotr.tekely@rmn.uhp-nancy.fr.
[†] Méthodologie RMN.
[‡] Chimie et Biochimie Théoriques.
[§] Chimie-Physique.

10.1021/jp062184v CCC: $33.50
Published on Web 07/04/2006

SCHEME 1: Three Successive Steps of Deprotonation and Corresponding Ionic Forms of *O*-Phosphoserine

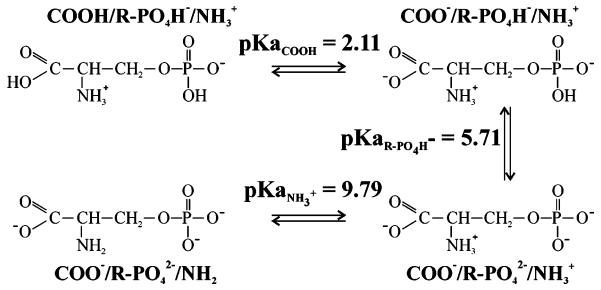

derived from low-speed MAS spectra using a homemade simulation program.

3. Computational Details. All calculations have been carried out with the quantum chemistry package Gaussian 98.[3] The DFT method used is the hybrid functional B3[4a] for the electronic quantum exchange and LYP[4b] for the electronic correlation, since it had been shown to produce reliable data at least for the carbon atom. Shielding constant tensors were evaluated by using the GIAO formalism.[5a−d] The convergence of the shielding constant values and of the principal axis orientation with respect to the basis set size was tested on model molecules CH_3COOH and $CH_3OPO_3H^-$ (see Supporting Information). The principal axis orientation is little dependent on the level of theory used since it mainly depends on the local symmetry around the nucleus under investigation. However, the largest basis set is required to describe as best as possible the shielding constant. Hence all calculations have been performed with the 6-311++G-(3d2f,3p2d) basis set. As the molecular geometry of lyophilized systems is not known, traditional techniques used to model the condensed phase are not adapted to the present case. The simulation protocol giving the best agreement between the experimental and calculated variations of the principal values of the shielding tensor was as follows. The experimental solid-state (X-ray) geometry[5e] of the $COOH/NH_3^+/PO_4H^-$ form was considered with the positions of the hydrogen atoms optimized at the HF/6-31G** level of theory. As X-ray data of deprotonated forms of L-phosphoserine are not yet available, it is impossible for the time being to consider accurate shift calculations taking into account the subtle effects due to the presence of hydrogen bonds involving different functional groups. Consequently, such intermolecular contacts were not modeled. The position of Na^+ counterion was optimized at the same level of theory in the vicinity of the phosphate group. GIAO calculations were carried out on this system embedded in a polarizable continuum[5f] to take into account the effects of the surroundings. This ensures a systematically much better agreement with experimental values and a proper sign of their changes as compared with the case of isolated molecule.

Results and Discussion

1. General Features of Carboxyl ^{13}C Chemical Shift Tensor Elements in Amino Acids. Chemical shift tensors of ^{13}C in carboxyl groups have been reported for a number of compounds, and their principal elements and orientations were found within relative narrow ranges.[6−9] The most shielded component δ_{33} was found systematically in the direction nearly perpendicular to the molecular COO plane, and the less shielded component δ_{11} was roughly along the C−C bond. Griffin et al.[6d,e] have compared the shift tensors of ionic and protonated carboxyl groups in ammonium hydrogen oxalate hemihydrate and have shown that protonation does not affect the shifts of the δ_{11} and δ_{33} tensor elements, but it does move the δ_{22} component in the direction of increased shielding (upfield shift) by about 8 ppm. A concurrent rotation of 25° about δ_{33} has been noted when going from the ionic to the protonated carboxyl group. More recently, Gu and McDermott[10] have shown that, in microcrystalline amino acids, the principal values δ_{11} and δ_{22} exhibit upon protonation shifts opposite in sign, compensating in this manner their contributions to the isotropic chemical shift value.

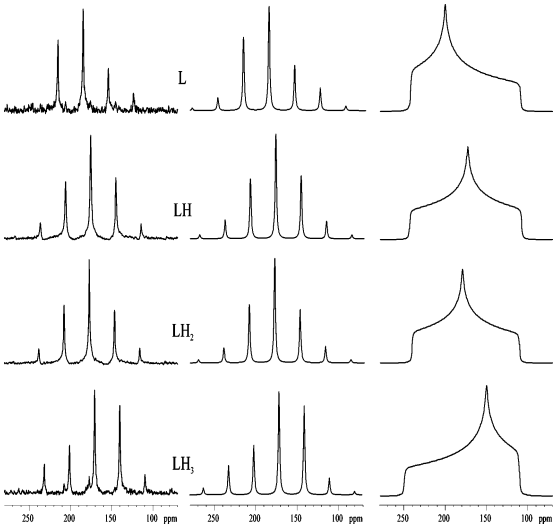

Figure 1. Experimental (left) and best-fitting simulated (middle) manifolds of ^{13}C CSA spinning sidebands of the carboxyl group in different ionic forms of L-histidine. The spinning frequency was 2.0 kHz. The corresponding simulated static powder spectra are also included (right).

The effects of hydrogen bonding on the ^{13}C chemical shift tensors were also reported in the literature.[11−13] Gu et al.[11] observed a strong correlation between the δ_{22} values and the length of hydrogen bonding. As expected from the deshielding effect of the deprotonation, for the protonated carboxyl groups, stronger hydrogen bonding leads to decreased shielding for the δ_{22} element while the reverse occurs for the deprotonated carboxylates. In the presence of fast hydrogen transfer between two hydrogen bonded conformers of benzoic acid, δ_{11} forms only a small angle with the C−C bond.[13] Slowing this transfer at low temperature leads to the increase of this angle up to 35°, which places δ_{22} approximately along the C═O bond. Moreover, some aspects of the relationship between ^{13}C principal elements of chemical shift tensors and the strength of hydrogen bonding in peptides and enantiomeric or racemic amino acids have been discussed in the literature.[14−17]

To introduce general spectroscopic features of the successive steps of deprotonation in amino acids as revealed by the carboxyl chemical shift principal values, experimental spectra for successive ionic forms of L-histidine have been recorded and analyzed as shown in Figure 1.

The principal values corresponding to each form are given in Table 1. The data visualize immediately the characteristic changes of the CSA resulting mainly from the downfield shift of the δ_{22} element after the deprotonation of carboxyl group ($LH_3 \rightarrow LH_2$) and amino group ($LH \rightarrow L$), and a smaller but significant upfield shift after the deprotonation of the imidazole ($LH_2 \rightarrow LH$). While the first +29 ppm and third, surprisingly high, +28 ppm downfield shifts are characteristic and dominant features of the deprotonation of the carboxyl group and neighboring amino group, the remaining −7 ppm upfield is due to the change in the intermolecular contacts after breaking the

TABLE 1: Experimental Principal Components (in ppm) of ^{13}C CSA Tensor of Carboxyl Carbon for Various Ionic Forms of L-Histidine[a]

ionic form	δ_{iso}	δ_{11}	δ_{22}	δ_{33}	δ_{aniso}	Ω	η
LH_3	170.7	251	151	111	80.3	140	0.50
LH_2	177.2	241	180	110	−67.2	131	0.90
LH	175.2	244	173	108	68.8	136	0.94
L	184.4	242	201	110	−74.4	132	0.55

[a] For definitions of anisotropy (δ_{aniso}), span (Ω), and asymmetry (η) parameters, see Table 2.

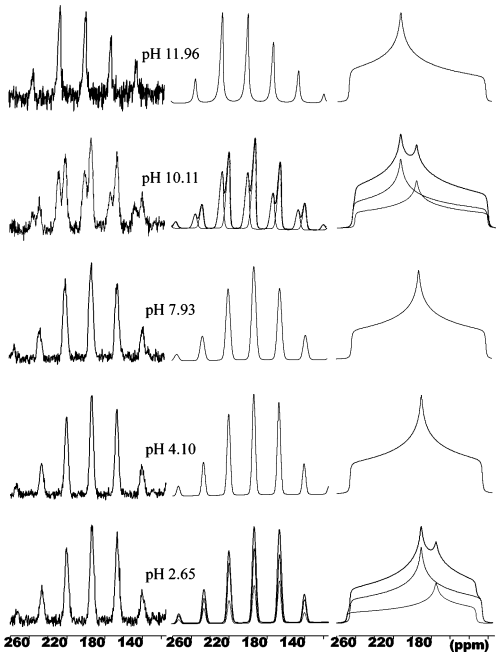

Figure 2. Experimental (left) and best-fitting simulated (middle) manifolds of ^{13}C CSA spinning sidebands of the carboxyl group in different ionic forms of L-phosphoserine. The spinning frequency was 2.0 kHz. The corresponding simulated static powder spectra are also included (right). Each of the simulated MAS and static spectra at pH 2.65 and 10.11 shows two components and their sums.

hydrogen bonding with the imidazole ring.[1a] Finally, contrary to such a high sensitivity of the δ_{22} element to deprotonation and hydrogen bonding, the δ_{11} principal value shows only −10 ppm upfield shift during the deprotonation of the carboxyl group.

2. Deprotonation of L-Phosphoserine As Revealed by the Carboxyl Chemical Shift Tensor. Figure 2 shows experimental families of ^{13}C spinning sidebands of carboxyl groups and the corresponding simulated spectra for lyophilisates prepared from solutions at different pH values encompassing three deprotonation steps of phosphoserine. The principal values δ_{ii} of the ^{13}C CSA carboxyl group in different ionic forms and their changes as a function of the pH are reported in Table 2 and shown in Figure 3. As expected for the lyophilisate prepared at pH 2.65, the presence of both protonated and deprotonated carboxyl groups has to be assumed in order to reproduce properly the observed envelope of spinning sidebands. The principal values of the chemical shift tensors of both forms were extracted first from corresponding spectra of powders where only a single form is present. The CSA of the protonated carboxyl group was obtained from the spectra of precipitated microcrystalline powders at pH between 1 and 2 (not shown) and is very close to that reported earlier in the literature.[10] The ratio of the fitted intensities in the bottom spectrum of Figure 2 allows calculation[1a] of the pK equal to 2.10−2.36 that is very close to the liquid-state values (2.04−2.19).

A similar situation occurs in the neighborhood of the deprotonation of the amino group, where a superposition of two species corresponding to NH_3^+ and NH_2 is clearly visible in the spectrum recorded at pH 10.11.

Figures 2 and 3 visualize immediately that, in analogy to L-histidine, the δ_{22} element of the carboxyl ^{13}C tensor of L-phosphoserine is very sensitive not only to the deprotonation of this group but also to the deprotonation step of the amide group.

A small but clear increase in the value of δ_{22} is also observed during the deprotonation of the phosphate group, which must be due to the breaking of hydrogen bonding involving both functional groups. This fully corroborates our previous findings of the sensitivity and direction of change of this principal value to the hydrogen bonding strength in the phosphorylated amino acids.[18]

The comparison between the experimental and calculated ^{13}C values of the principal tensor elements for successive ionic forms of L-phosphoserine is given in Table 2. A satisfactory agreement is noted in the amount and direction of deprotonation-induced changes of the δ_{22} element, showing its dominant sensitivity to the intramolecular effect of deprotonation of the carboxyl and amide groups. Some minor divergences also noted for two other principal values come most probably from the modification in the intermolecular interactions not taken into account in the calculations.

To probe the directional sensitivity of the chemical shift tensor, one needs to consider additionally its orientation with respect to the molecular frame. Table 3 gives the angles of the principal axes of the shielding tensor of carboxyl carbon calculated for the successive ionic forms, while Figure 4 visualizes its reorientation with respect to the COO molecular plane, after the deprotonation of the carboxyl group. The data from Table 3 show that the δ_{11} element placed in the COO plane ($\alpha_1 + \alpha_2 = -O{=}C{-}O$) moved in this plane toward the C−C direction after carboxyl deprotonation ($\alpha_1 + -C{-}C{-}O = \alpha_2 + -O{=}C{-}C$, both close to 180°). This change is due to the rotation of the tensor around the axis perpendicular to the COO plane by about 30°. Moreover, this ionization step is accompanied by a second, less than 5° rotation around the δ_{11} axis, which moves the δ_{22} element toward the COO plane and increases the angle between the C=O direction and δ_{33} axis. Equally interesting, the deprotonation of the amide group, leading to a 20 ppm downfield shift of the δ_{22} principal value, is accompanied only by a small rotation around the axis perpendicular to the COO plane and of opposite direction than the rotation due to carboxyl deprotonation. The large amplitude rotation of the tensor around the axis perpendicular to the COO plane accompanying the carboxyl deprotonation is quite universal, as shown on the model molecule CH_3COOH (see Supporting Information) and reported previously experimentally on a small number of monocrystalline systems.[6d,e] The change in site symmetry around the carboxylic carbon atom when going from protonated (C_s) to deprotonated (C_{2v}) forms is responsible for the reorientation of the principal axis of the tensor. This reorientation seems to be the main reason for different changes of the δ_{ii} principal values as concluded from similar shielding of both forms (see Supporting Information). The deprotonation of the amino group does not change the site symmetry around the carboxylate atom, and the principal axis orientation is only slightly modified. However, the 20 ppm downfield shift clearly indicates a modification of the shielding in the δ_{22} direction, which is certainly due to a change of the interaction between the carboxylate moiety and the NH_3^+ group.

TABLE 2: Experimental[a] and Calculated ^{13}C Values of the Principal Tensor Elements δ_{ii} and Corresponding Anisotropic Parameters of Carboxyl Carbon for Various Ionic Forms of L-Phosphoserine

		^{13}C carboxyl data						
ionic form		δ_{iso} (ppm)	δ_{11} (ppm)	δ_{22} (ppm)	δ_{33} (ppm)	δ_{aniso} (ppm)	Ω (ppm)	η
$COOH/NH_3^+/PO_4H^-$	experimental[b]	171.7	250	150	115	78.3	135	0.45
	calculated	178.7	273	154	109	94.3	164	0.48
$COO^-/NH_3^+/PO_4H^-$	experimental[c]	174.0	245	170	107	71.0	138	0.89
	calculated	183.3	273	163	114	89.7	159	0.55
	Δ experimental	2.3	−5	+20	−8			
	Δ calculated	4.6	0	+9	+5			
$COO^-/NH_3^+/PO_4^{2-}$	experimental[d]	175.3	244	175	107	68.7	137	0.99
	calculated	179.7	261	165	113	81.3	148	0.64
	Δ experimental	1.3	−1	+5	0			
	Δ calculated	−3.6	−12	+2	−1			
$COO^-/NH_2/PO_4^{2-}$	experimental[e]	182.7	246	195	107	−75.7	139	0.67
	calculated	188.0	256	196	112	−76.0	144	0.79
	Δ experimental	7.4	+2	+20	0			
	Δ calculated	8.3	−5	+31	−1			

[a] Estimated errors in δ_{11}, δ_{22}, and δ_{33} are ±3 ppm; span is expressed as $\Omega = \delta_{11} - \delta_{33}$; anisotropy is calculated as $\delta_{aniso} = \delta_{33} - \delta_{iso}$ and asymmetry as $\eta = (\delta_{22} - \delta_{11})/(\delta_{33} - \delta_{iso})$ when $|\delta_{11} - \delta_{iso}| \leq |\delta_{33} - \delta_{iso}|$ or $\delta_{aniso} = \delta_{11} - \delta_{iso}$ and $\eta = (\delta_{22} - \delta_{33})/(\delta_{11} - \delta_{iso})$ when $|\delta_{11} - \delta_{iso}| \geq |\delta_{33} - \delta_{iso}|$; Δ = difference due to the corresponding ionization. [b−e] Average values from the corresponding range of the pH. To convert the shielding constants into the chemical shifts, the δ_{ref} was chosen to be 184.2 ppm obtained with the same DFT basis as in the main calculations.

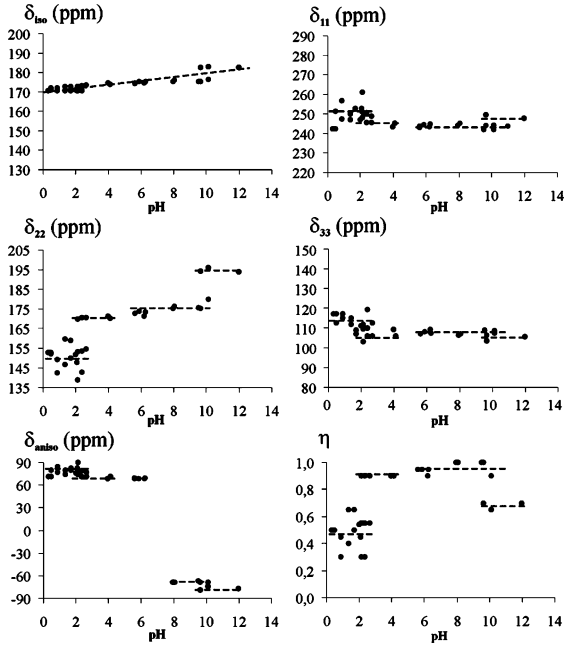

Figure 3. Changes of the isotropic chemical shift δ_{iso}, the principal values δ_{ii}, and the anisotropy (δ_{aniso}) and asymmetry (η) parameters of the ^{13}C CSA tensor of the carboxyl group in L-phosphoserine as a function of pH. The anisotropy and asymmetry parameters have their usual meaning (see Table 2).

TABLE 3: DFT-Based Orientation of the Principal Axes of Shielding Tensor of Carboxyl Carbon for Various Ionic Forms of L-Phosphoserine[a]

ionic form	α_1	α_2	β_1	β_2	γ_1	γ_2
$COOH/NH_3^+/PO_4H^-$	32.7	93.6	122.6	7.7	92.0	83.2
$COO^-/NH_3^+/PO_4H^-$	63.8	62.4	153.6	27.8	93.0	87.1
$COO^-/NH_3^+/PO_4^{2-}$	63.8	62.4	153.6	27.8	92.8	87.3
$COO^-/NH_2/PO_4^{2-}$	59.3	66.9	149.2	23.2	92.2	87.8
−O=C−C	121.5		−C−C−O		112.3	
−O=C−O	126.2					

[a] For the definition of angles, see Figure 4.

3. General Features of the Phosphate ^{31}P Chemical Shielding Tensor in Phosphorylated Amino Acids. The orientation of the principal axis of ^{31}P shielding tensor in isolated molecules of phoshorylated amino acids is close to the orientation found in the case of $H_2PO_4^-$ molecule.[18] This orientation is shown in Figure 5.

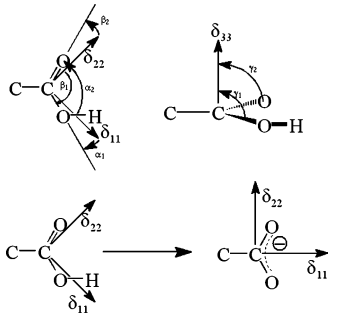

Figure 4. DFT-based ^{13}C chemical shielding tensor orientation angles (top) of the carboxyl group and its changes when going from its protonated (bottom left) to deprotonated (bottom right) form (also see Table 3).

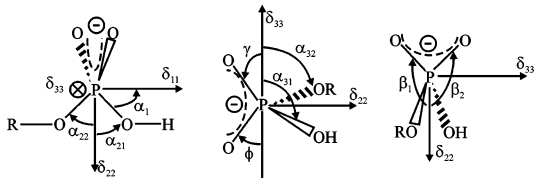

Figure 5. ^{31}P chemical shielding tensor orientation in O-phosphorylated amino acids.[18]

The principal axes of δ_{11} and δ_{22} elements have been found in a plane perpendicular to the O=P−O$^-$ plane. The axis corresponding to δ_{22} element nearly bisects the O(R)−P−O(H) angle. This axis also nearly bisects the O=P−O$^-$ angle. The δ_{33} axis is almost perpendicular to the O(R)−P−O(H) plane. The same axis is also in the O=P−O$^-$ plane. Attempts were made before to correlate δ_{33} with structural parameters of a wide variety of phosphate-bearing compounds.[19,20] It was suggested that the observed differences of this element can reflect the changes in O=P−O valence angles or in an average length of shortest P−O bonds.[19] However, no such correlation has been observed for O-phosphorylated amino acids.[18] On the other hand, important changes of the principal values and orientation of ^{31}P chemical shielding tensor in the presence of hydrogen bonds involving the phosphate group in O-phosphorylated amino acids have been observed.[18] Opposite trends in the changes of the principal components of the ^{31}P shielding tensor for L and

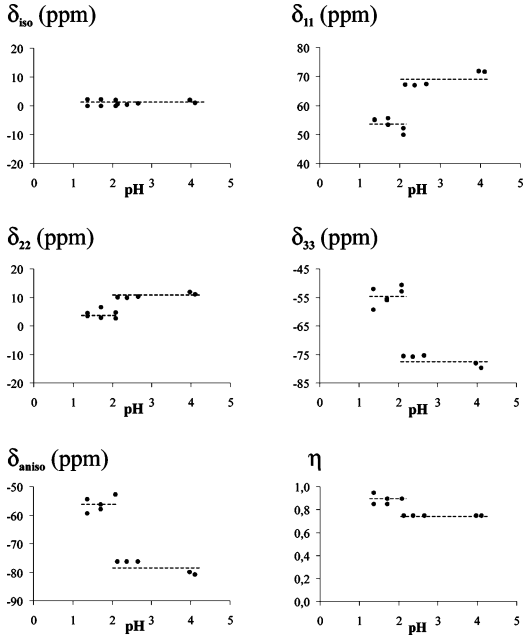

Figure 6. Changes of the isotropic chemical shift δ_{iso}, the principal values δ_{ii}, and the anisotropy (δ_{aniso}) and asymmetry (η) parameters of the ^{31}P CSA tensor of the phosphate group in L-phosphoserine as a function of pH covering the deprotonation region of the carboxyl group.

DL forms as a function of hydrogen bond distance have been related to different natures of the shortest hydrogen bonds with the phosphate group behaving as an acceptor and as a donor/acceptor, respectively. This manifests itself by opposite changes of principal components and of corresponding anisotropic parameters and may be related to opposite rotations of the ^{31}P shielding tensor upon changes in the hydrogen bonding strength. Indeed, on the basis of the theoretical calculations, it has been revealed that the presence of hydrogen bonding leads to significant reorientation of the ^{31}P shielding tensor around the axis of the δ_{22} and δ_{33} elements.[18]

3.1. Deprotonation of the Carboxyl Group As Revealed by the Phosphate ^{31}P Chemical Shift Tensor. To understand the role played by the phosphate functional group in catalytic events or in protein structure formation, one needs to answer the question of whether the phosphate group is mono- or dianionic and to what extent its ionization state is affected by the presence of ligands or changes in the intermolecular contacts involving hydrogen bonding. The changes of the ^{31}P principal elements δ_{ii} and anisotropy (δ_{aniso}) and asymmetry (η) parameters as a function of the pH covering the deprotonation region of the carboxyl group are reported in Figure 6. The δ_{33} element shows the most pronounced sensitivity to the ionization of the carboxyl group leading to the decrease of its value by about 20 ppm, while the δ_{11} and δ_{22} values increase respectively by about 15 and 5 ppm. This is responsible for a fortuitous constancy of the value of δ_{iso} for ^{31}P during this ionization step. The decrease of the δ_{33} value and increase of δ_{11} and δ_{22} values are directly related to the breaking of strong hydrogen bonding contact involving both functional groups and fully confirm previously reported, experimentally observed and theoretically reproduced opposite shifts of the δ_{33} and δ_{22} principal values due to the changes in the strength of hydrogen bonding.[18]

3.2. Secondary Ionization of the Phosphate Group. The issue of whether a phosphate group is mono- or dianionic is of prime importance when studying the activation of biomolecules. As shown in Figure 7, this question can be answered in a straightforward manner by using solid-state ^{31}P NMR through

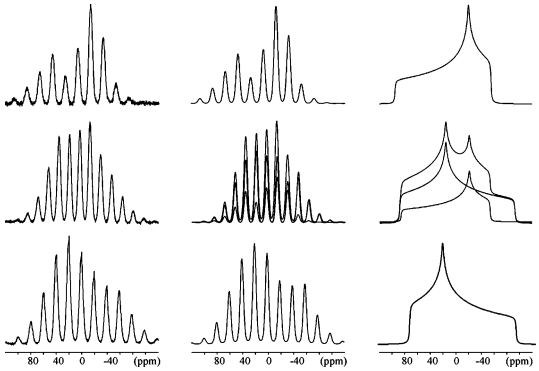

Figure 7. Experimental (left) and the best-fitting simulated (middle) manifolds of ^{31}P CSA spinning sidebands of the phosphate group in L-phosphoserine lyophilisates prepared at pH 2.65 (bottom), pH 5.61 (middle), and pH 7.93 (top). The spinning frequency was 2.0 kHz. The corresponding simulated static powder spectra are also included (right). The simulated MAS and static spectra at pH 5.61 show two components and their sums.

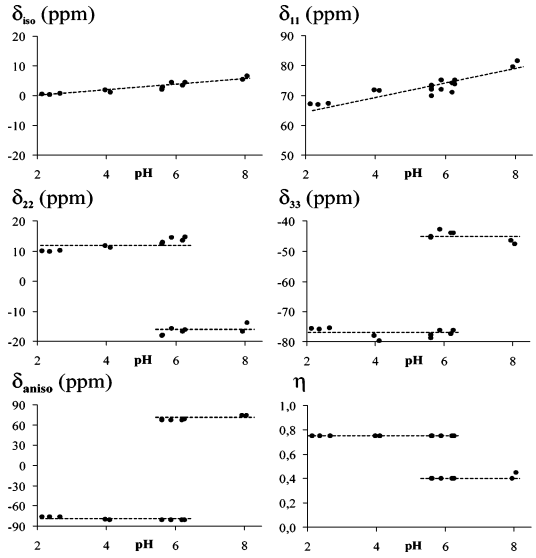

Figure 8. Changes of the isotropic chemical shift δ_{iso}, the principal values δ_{ii}, and the anisotropy (δ_{aniso}) and asymmetry (η) parameters of the ^{31}P CSA tensor as a function of pH close to the secondary ionization of the phosphate group in L-phosphoserine.

the characteristic effect of the secondary ionization of the phosphate group on the form of the ^{31}P CSA tensor. The changes of the principal elements δ_{ii} and anisotropy and asymmetry parameters as a function of the pH covering the secondary ionization region of the phosphate group in L-phosphoserine are reported in Figure 8 (see also Table 4). In contrast to a continuous increase of δ_{iso} and δ_{11}, the second ionization of phosphate leads to a dramatic jump in opposite directions of δ_{22} and δ_{33} values. A second striking feature of these changes is related to the opposite directions of these changes as compared with the changes due to disruption of hydrogen bonding during the deprotonation of the carboxyl group. This is related to a specific sensitivity of the principal axes because of their particular orientation in the molecular frame of the phosphate group. As shown in Figure 9, fully corroborating experimental evidence revealing common trends of ^{31}P CSA changes upon the protonation state can be observed in two other phosphorylated systems such as adenosine monophosphate-5′ (AMP-5′) and glucose-6-phosphate.

From the simulations of spinning sideband manifolds in the range of secondary ionization where both mono- and dianionic species are present simultaneously, we have determined the

TABLE 4: Experimental[a] and Calculated ^{31}P Values of the Principal Tensor Elements δ_{ii} and Corresponding Anisotropic Parameters for Various Ionic Forms of L-Phosphoserine

		^{31}P phosphate data						
ionic form		δ_{iso} (ppm)	δ_{11} (ppm)	δ_{22} (ppm)	δ_{33} (ppm)	δ_{aniso} (ppm)	Ω (ppm)	η
$COOH/NH_3^+/PO_4H^-$	experimental[b]	0.6	53	4	−55	−56	108	0.88
	calculated	−3.6	81	6	−98	−94	179	0.80
$COO^-/NH_3^+/PO_4H^-$	experimental[c]	1.1	72	11	−76	−81	152	0.75
	calculated	−3.1	79	6	−94	−93	173	0.79
$COO^-/NH_3^+/PO_4^{2-}$	experimental[d]	3.5	71	−17	−44	67	115	0.40
	calculated	0.3	82	−22	−59	82	141	0.45
	Δ experimental	+2.4	−1	−28	+32			
	Δ calculated	+1.6	+3	−28	+35			
$COO^-/NH_2/PO_4^{2-}$	experimental[e]	8.4	80	−14	−45	72	125	0.43
	calculated	0.6	78	−20	−56	77	134	0.47

[a] Estimated errors in δ_{11}, δ_{22}, δ_{33} are ±3 ppm; span is expressed as $\Omega = \delta_{11} - \delta_{33}$; anisotropy is calculated as $\delta_{aniso} = \delta_{33} - \delta_{iso}$ and asymmetry as $\eta = (\delta_{22} - \delta_{11})/(\delta_{33} - \delta_{iso})$ when $|\delta_{11} - \delta_{iso}| \leq |\delta_{33} - \delta_{iso}|$ or as $\delta_{aniso} = \delta_{11} - \delta_{iso}$ and $\eta = (\delta_{22} - \delta_{33})/(\delta_{11} - \delta_{iso})$ when $|\delta_{11} - \delta_{iso}| \geq |\delta_{33} - \delta_{iso}|$; Δ = difference due to the secondary ionization. [b−e] Average values from the corresponding range of the pH. To convert the shielding constants into the chemical shifts the δ_{ref} was chosen to be 287.3 ppm obtained with the same DFT basis as in the main calculations.

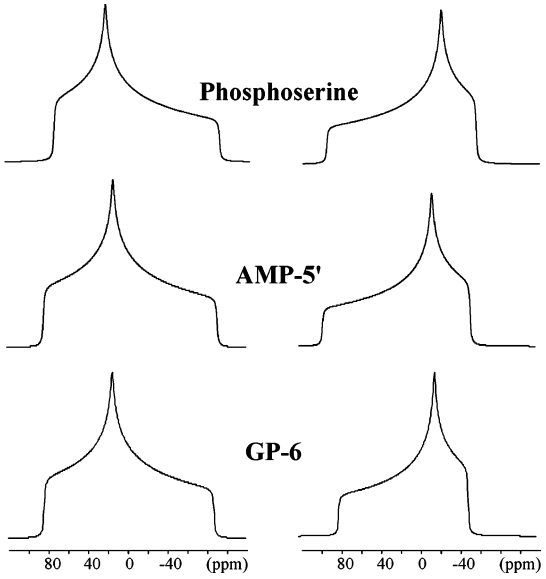

Figure 9. Reconstruction of ^{31}P CSA powder spectra of monoanionic (left) and dianionic (right) phosphate group in lyophilisates of L-phosphoserine, AMP-5′ and GP-6 prepared with NaOH.

ratios of the amounts of both forms, which as mentioned above permits calculation of the p*K* values. For phosphoserine, AMP-5′, and glucose-6-phosphate, respectively, the average pK_2 values of 5.9, 6.42, and 6.35 have been obtained, and are only slightly larger than the corresponding average values of 5.7, 6.2, and 6.0 measured in solution.

The observed changes of the principal values accompanying the secondary ionization of the phosphate group in L-phosphoserine are compared with the theoretical calculations in Table 4. An excellent agreement between the experimental (−28 and +32 ppm) and calculated (−28 and +35 ppm) changes of δ_{22} and δ_{33} principal values has been obtained. This witnesses that the electronic changes occurring during secondary ionization of the phosphate group are adequately defined in the theoretical calculations.

Finally, the concurrent change in the orientation of the chemical shielding tensor upon this deprotonation deserves a comment. Table 5 gives the angles of the principal axes of ^{31}P shielding tensor calculated for the successive ionic forms.

These data show that the secondary ionization of the phosphate group leads to a significant change of the orientation of the ^{31}P shielding tensor which consists of a small amplitude rotation around the δ_{11} direction and a second rotation of about

TABLE 5: DFT-Based Orientation of the Principal Axes of Shielding Tensor of Phosphate for Various Ionic Forms of L-Phosphoserine[a]

ionic form	α_1	α_{21}	α_{22}	α_{31}	α_{32}
$COOH/NH_3^+/PO_4H^-$	47.0	43.1	58.5	88.8	90.4
$COO^-/NH_3^+/PO_4H^-$	45.6	44.4	57.1	88.8	90.5
$COO^-/NH_3^+/PO_4^{2-}$	71.3	18.7	82.9	91.3	92.5
$COO^-/NH_2/PO_4^{2-}$	70.7	19.5	82.4	92.3	93.0

ionic form	β_1	β_2	γ	ϕ
$COOH/NH_3^+/PO_4H^-$	122.0	122.9	32.1	33.0
$COO^-/NH_3^+/PO_4H^-$	122.0	123.0	32.1	33.1
$COO^-/NH_3^+/PO_4^{2-}$	114.4	121.2	28.5	36.7
$COO^-/NH_2/PO_4^{2-}$	113.5	122.6	27.3	37.9

$-O{=}P-O^-$ 114.8 $-O(Me)-P-O(H)$ 101.4

[a] For the definition of angles, see Figure 5.

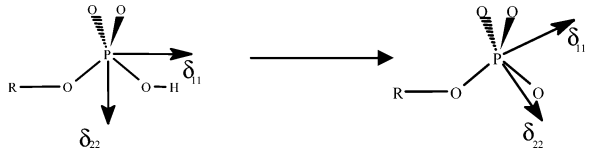

Figure 10. DFT-based rotation of the ^{31}P chemical shielding tensor of the phosphate group due to its secondary ionization.

25° around the new δ_{33} direction. This second rotation is illustrated in Figure 10.

While this first, small amplitude rotation leads to the displacement of δ_{33} element in the $O{=}P-O^-$ plane, the second rotation moves the σ_{22} axis out of this plane.

3.3. Effect of Counterions on the Principal Values of the ^{13}P Chemical Shift Tensor. Alkali metal cations binding to biomolecules play an important role in their biological activity and contribute to the stability of the intermolecular contacts through the ion−multipole interactions. Precise information about the charge of the phosphate groups in a complex molecular environment is indeed crucial for understanding the involvement of this group in catalytic events and in protein formation. Here we wish to compare the electronic effects of Li^+, Na^+, and K^+ counterions on the principal values of the ^{31}P tensor of the phosphate group and to check to what extent these effects could influence the characteristic fingerprints of deprotonation revealed by the opposite shifts of the δ_{22} and δ_{33} principal values.

Figure 11 shows the static CSA spectra simulated from the fitted manifolds of ^{31}P spinning sidebands of lyophilisates prepared with LiOH, NaOH, and KOH at a pH value close to p$K_{HPO_4^-}$. The characteristic change of the CSA pattern due to

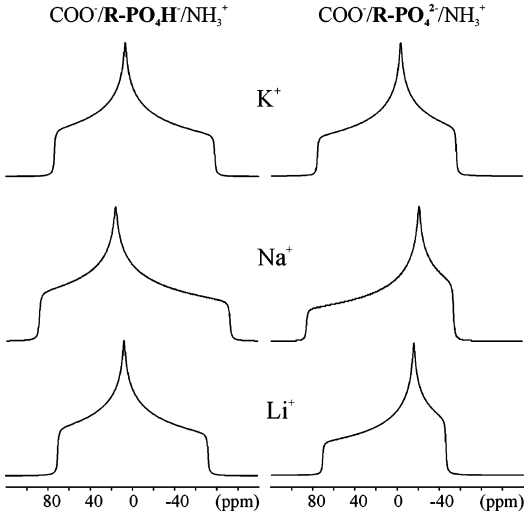

Figure 11. Reconstruction of ^{31}P CSA powder spectra of monoanionic (left) and dianionic (right) phosphate groups in lyophilisates of L-phosphoserine prepared with LiOH, NaOH, and KOH.

the secondary ionization of the phosphate group is indeed clearly observed in each case. However, distinct differences in the individual principal values may be noted. The main difference comes from the more pronounced, deprotonation-induced changes of the δ_{22} and δ_{33} principal values in the presence of Li^+ and Na^+ cations, which we attribute to their smaller size permitting closer distance to the phosphate groups. This must lead itself to a disruption of their intermolecular contacts through hydrogen bonding. Moreover, we have observed the important change of the phosphate δ_{33} principal value during the deprotonation of the NH_3 group only in the presence of K^+, while the same deprotonation could not be detected via the carboxyl in the presence of this cation. This indicates the spatial emplacement of K^+ close to the carboxyl group and of Na^+ as well as Li^+ cations in the neighborhood of the phosphate group.

Conclusions

We have detected and analyzed the solid-state spectroscopic fingerprints from the chemical shift tensors upon successive steps of deprotonation of L-phosphoserine. The data as a whole provide a novel, strong support of our recent findings[1] of the exceptional suitability of the ^{13}C and ^{31}P chemical shift tensors to follow successive deprotonations of different functional groups.

DFT calculations of the chemical shielding tensors upon deprotonation have been carried out for the first time. The calculations on successive ionic forms embedded in a polarizable continuum, taking into account the global surroundings effects, showed not only their ability to reproduce experimentally observed changes due to the intramolecular electronic shielding modifications, but also provided for the first time the precious information about the concurrent changes in the orientation of the chemical shielding tensors occurring due to site symmetry changes. Such changes of orientation, very difficult to access experimentally, have been previously reported in only a couple of solid-state NMR studies on some monocrystalline systems.[6d,e,13]

The minor experimental changes in the principal values due to deprotonation-induced modifications in the intermolecular contacts have been related to the breaking of hydrogen bonding. These subtle effects remain for the moment impossible to handle in the DFT calculations for a lyophilized powder.

The measurements of ^{31}P chemical shift tensor are especially well suited to access the characteristic spectroscopic features related to singly and doubly ionized phosphate groups in lyophilisates prepared from parent solutions at different pH values. Although distinct differences in the individual principal values may be observed in the presence of Li^+, Na^+, and K^+ cations, the characteristic change of the CSA pattern due to the secondary ionization of the phosphate group is clearly visible in each case.

Finally, it is worth pointing out that liquid-state alternative, i.e., pH titration with observation of one-dimensional ^{13}C and ^{31}P spectra, could not provide such straightforward information about the ionization state not only due to disadvantageous rapid proton exchanges but also, as demonstrated in this work, due to largely canceling opposite shifts of individual principal values in the trace of a chemical shift tensor.

Acknowledgment. This work was supported by a research award (BQR) from Université H. Poincaré, Nancy 1.

Supporting Information Available: Tables of principal components of the shielding tensors with respect to the basis set size. Shielding densities of protonated and deprotonated carboxyl group. This material is available free of charge via the Internet at http://pubs.acs.org.

References and Notes

(1) (a) Henry, B.; Tekely, P.; Delpuech, J. J. *J. Am. Chem. Soc.* **2002**, *124*, 2025. (b) Colsenet, R.; Gardiennet, C.; Henry, B.; Tekely, P. *Angew. Chem., Int. Ed. Engl.* **2002**, *24*, 4743. (c) Gardiennet, C.; Henry, B.; Kuad, P.; Spiess, B.; Tekely, P. *Chem. Commun.* **2005**, 180−182.

(2) Tekely, P.; Palmas, P.; Canet, D. *J. Magn. Reson., A* **1994**, *107*, 129.

(3) Frisch, M. J.; Trucks, G. W.; Schlegel, H. B.; Scuseria, G. E.; Robb, M. A.; Cheeseman, J. R.; Zakrzewski, V. G.; Montgomery, J. A., Jr.; Stratmann, R. E.; Burant, J. C.; Dapprich, S.; Millam, J. M.; Daniels, A. D.; Kudin, K. N.; Strain, M. C.; Farkas, O.; Tomasi, J.; Barone, V.; Cossi, M.; Cammi, R.; Mennucci, B.; Pomelli, C.; Adamo, C.; Clifford, S.; Ochterski, J.; Petersson, G. A.; Ayala, P. Y.; Cui, Q.; Morokuma, K.; Malick, D. K.; Rabuck, A. D.; Raghavachari, K.; Foresman, J. B.; Cioslowski, J.; Ortiz, J. V.; Baboul, A. G.; Stefanov, B. B.; Liu, G.; Liashenko, A.; Piskorz, P.; Komaromi, I.; Gomperts, R.; Martin, R. L.; Fox, D. J.; Keith, T.; Al-Laham, M. A.; Peng, C. Y.; Nanayakkara, A.; Gonzalez, C.; Challacombe, M.; Gill, P. M. W.; Johnson, B.; Chen, W.; Wong, M. W.; Andres, J. L.; Gonzalez, C.; Head-Gordon, M.; Replogle, E. S.; Pople, J. A. *Gaussian 98*, revision A.7; Gaussian, Inc.: Pittsburgh, PA, 1998.

(4) (a) Becke, A. D. *J. Chem. Phys.* **1993**, *98*, 5648. (b) Lee, C.; Yang, W.; Parr, R. G. *Phys. Rev. B* **1988**, *37*, 785.

(5) (a) Helgaker, T.; Jaszunski, M.; Ruud, K. *Chem. Rev.* **1999**, *99*, 293. (b) Rich, J. E.; Manalo, M. N.; de Dios, A. C. *J. Phys. Chem. A* **2000**, *104*, 5837. (c) Ditchfield, R. *Mol. Phys.* **1974**, *27*, 789. (d) Wolinski, K.; Hinton, J. F.; Pulay, P. *J. Am. Chem. Soc.* **1990**, *112*, 8251. (e) The experimental geometry was retrieved from the Centre for Molecular and Biomolecular Informatics facilities, University of Nijmegen, The Netherlands. (f) Rinaldi, D.; Bouchy, A.; Rivail, J.-L.; Dillet, V. J. *Chem. Phys.* **2004**, *120*, 2343. Rinaldi, D.; Pappalardo, R. R. *SCRFPAC*; Quantum Chemistry Program Exchange; Indiana University: Bloomington, IN, 1992; Program No. 622 (the relative dielectric constant was fixed to 78).

(6) (a) Chang, J. J.; Griffin, R. G.; Pines, A. *J. Chem. Phys.* **1974**, *60*, 2561. (b) Ackerman, J. L..; Tegenfeld, J.; Waugh, J. S. *J. Am. Chem. Soc.* **1974**, *96*, 6843. (c) Pines, A.; Chang, J. J.; Griffin, R. G. *J. Chem. Phys.* **1974**, *61*, 1021. (d) Griffin, R. G.; Pines, A.; Pausak, S.; Waugh, J. S. *J. Chem. Phys.* **1975**, *63*, 1267. (e) Griffin, R. G.; Ruben, D. J. *J. Chem. Phys.* **1975**, *63*, 1272.

(7) Kempf, J.; Spiess, H. W.; Haeberlen, U.; Zimmerman, H. *Chem. Phys.* **1974**, *4*, 269.

(8) Veeman, W. S. *Prog. NMR Spectrosc.* **1984**, *16*, 193.

(9) Separovic, F.; Smith, R.; Yannoni, C. S.; Cornell, B. A. *J. Am. Chem. Soc.* **1990**, *112*, 8324.

(10) Gu, Z.; McDermott, A. *J. Am. Chem. Soc.* **1993**, *115*, 4282.

(11) Gu, Z.; Zambrano, R.; McDermott, A. *J. Am. Chem. Soc.* **1994**, *116*, 6368.

(12) Ando, S.; Ando, I.; Shoji, A.; Ozaki, T. *J. Am. Chem. Soc.* **1988**, *110*, 3380.

(13) Nagaoka, S.; Terao, T.; Imashiro, F.; Saika, A.; Hirota, N. *Chem. Phys. Lett.* **1981**, *80*, 580.

(14) Wei, Y.; de Dios, A. C.; McDermott, A. E. *J. Am. Chem. Soc.* **1999**, *121*, 10389.

(15) Potrzebowski, M. J.; Schneider, C.; Tekely, P. *Chem. Phys. Lett.* **1999**, *313*, 569.

(16) (a) Sitkoff, D.; Case, D. A. *Prog. Nucl. Magn. Reson. Spectrosc.* **1998**, *32*, 165−190. (b) Antzutkin, O. N. Molecular Structure Determination: Application in Biology. In *Solid State NMR spectroscopy*—principles and applications; Duer, M. J., Ed.; Blackwell Science: Cambridge, MA, 2002; Chapter 7, pp 280−390.

(17) (a) Wei, Y.; Lee, D.-K.; Ramamoorthy, A. *J. Am. Chem. Soc.* **2001**, *123*, 6118. (b) Brender, J. R.; Taylor, D. M.; Ramamoorthy, A. *J. Am. Chem. Soc.* **2001**, *123*, 914. (c) Lee, D.-K.; Wei, Y.; Ramamoorthy, A. *J. Phys. Chem. B* **2001**, *105*, 4752.

(18) Potrzebowski, M. J.; Assfeld, X.; Ganicz, K.; Olejniczak, S.; Cartier, A.; Gardiennet, C.; Tekely, P. *J. Am. Chem. Soc.* **2003**, *125*, 4223.

(19) Un, S.; Klein, M. P. *J. Am. Chem. Soc.* **1989**, *111*, 5119.

(20) Larsson, A.-C.; Ivanov, A. V.; Forsling, W.; Antzutkin, O. N.; Abraham, A. E.; de Dios, A. C. *J. Am. Chem. Soc.* **2005**, *127*, 2218.